SRYAHWA PUBLICATIONS

Open Access Journal of Physics
ISSN: 2637-5826 | Volume 8, Issue 4, 2026
https://doi.org/10.22259/2637-5826.0804002

RESEARCH ARTICLE

A Causal Anti-Calculus Memory-Kernel Model for Viscoelastic Non-Newtonian Turbulence

Begüm Yıldırım

Department of Molecular Biology and Genetics, Faculty of Engineering and Natural Sciences, Üsküdar University, Istanbul, Türkiye.

Received: 10 August 2026 Accepted: 29 October 2026 Published: 12 November 2026

Corresponding Author: Begüm Yıldırım, Department of Molecular Biology and Genetics, Faculty of Engineering and Natural Sciences, Üsküdar University, Istanbul, Türkiye.

Abstract

Non-Newtonian turbulence in polymeric and viscoelastic liquids involves an interaction between the velocity field, constitutive memory, elastic energy storage, dissipation, and multi-scale transfer. This manuscript develops a causal Anti-Calculus-inspired constitutive extension (AC-NNNS) and tests its principal mechanisms and an exploratory relaxation/crossover scaling against external experimental literature. The mathematical starting point is the supplied Anti-Calculus framework, which defines reverse accumulation through sign-reversed derivative/integral operations. A new causal extension is introduced here by applying a history operator to the rate-of-strain tensor. For a normalized kernel K(tau), the memory field is A_K[D](t)=∫K(tau)[D(t-tau)-D(t)]d tau, and the extra stress is taken as tau_A=2 eta_A A_K[D]. The contribution -tau_A:D to the kinetic-energy equation is sign-indefinite, permitting the same constitutive channel to act locally either as an energy sink or as a return pathway from stored elastic energy to fluid motion. This feature is consistent with external experiments showing both polymeric energy dissipation and random release of stored elastic energy into velocity fluctuations. A two-relaxation exponential kernel is then introduced to represent multiple molecular/time scales. Quantitative comparison uses two microchannel experiments. The conclusions are limited to the stated model, dataset, and assumptions; the analysis does not establish the proposed mechanism as unique or experimentally confirmed.

Keywords: Non-Newtonian Turbulence, Viscoelastic Turbulence, Elastic Turbulence, Polymer Solutions, Constitutive Memory.

1. Introduction and Theoretical Framework

1.1 Anti-Calculus Source Framework

The supplied theoretical manuscript, Anti-Calculus: A Formal Axiomatic Framework, defines Anti-Calculus as a reverse-operator construction relative to classical calculus. Its central ingredients include an anti-accumulation rule T(f')=-f+C, an anti-limit obtained through sign reversal, reverse-integral symmetry, and an anti-derivative expressed through a sign-reversed integral of a derivative. The source manuscript proposes possible connections to reversed temporal flow, anti-dissipative systems, and negative entropy-flow descriptions. These definitions are used only as the conceptual mathematical starting point in the present paper.

The causal rheological memory kernel derived below is not contained in the source manuscript. It is a new constitutive extension constructed in the present work so that the reverse-accumulation idea can be tested against measured viscoelastic-flow phenomena.

Citation: Begüm Yıldırım, A Causal Anti-Calculus Memory-Kernel Model for Viscoelastic Non-Newtonian Turbulence. Open Access Journal of Physics. 2026;8(4): 04-13.

©The Author(s) 2026. This is an open access article distributed under the Creative Commons Attribution License, which permits unrestricted use, distribution, and reproduction in any medium, provided the original work is properly cited.

Source role	Status in present paper
Anti-accumulation / anti-derivative definitions	Taken from supplied Anti-Calculus manuscript
Causal strain-history operator	New extension introduced here
AC-NNNS momentum equation	New constitutive model introduced here
Multi-relaxation kernel	New extension introduced here
External experimental tests	Performed here from published literature values

1.2 Why Causality Matters

A physical constitutive law for ordinary laboratory fluids must not depend on future strain. Therefore a literal integration from the future toward the present is replaced by a causal history operator whose sign and differencing structure preserve the intended reverse-accumulation interpretation while using only past states.

$$A_K[D](t) = \int_0^\infty K(\tau)\,[\,D(t-\tau) - D(t)\,]\,d\tau$$

The kernel K(tau) is normalized and non-negative in the basic model, so A_K has the same dimensions as the rate-of-strain tensor D. For a single finite window this reduces to a delayed difference; for an exponential kernel it becomes a smooth causal memory.

2. Baseline Non-Newtonian Momentum Balance

$$\nabla \cdot u = 0$$

$$\rho(\partial_t u + u \cdot \nabla u) = -\nabla p + \nabla \cdot (\tau_{NN} + \tau_A) + f$$

For a generalized-Newtonian baseline,

$$\tau_{NN} = 2\eta_{eff}(\dot\gamma)\,D$$

$$D = (\nabla u + \nabla u^T)/2$$

$$\dot\gamma = \sqrt{2\,D:D}$$

For example, a power-law fluid uses $\eta_{eff}=K_{PL}\dot\gamma^{(n-1)}$. The AC term is added to, rather than substituted for, the conventional constitutive stress:

$$\tau_A = 2\eta_A A_K[D]$$

Here eta_A is a material coupling scale with viscosity units. The construction can also be combined with more sophisticated baseline constitutive equations.

3. Energy Budget and Sign-Indefinite Exchange

Multiplying the momentum equation by u and integrating over a closed or suitably periodic domain gives a kinetic-energy balance of the form:

$$dE_k/dt = P_{in} - \int \tau_{NN}:D\,dV - \int \tau_A:D\,dV$$

For dissipative generalized-Newtonian stresses, $\tau_{NN}:D$ is non-negative. The Anti-Calculus memory term is different because $A_K[D]$ can be aligned or anti-aligned with the current D:

$$\Pi_A = -\tau_A : D$$

$\Pi_A>0$ corresponds to a positive contribution to the instantaneous kinetic-energy rate; $\Pi_A<0$ corresponds to an additional sink. This does not create energy from nothing: in a physically complete viscoelastic interpretation, positive Π_A represents return of previously stored elastic energy, while negative Π_A represents transfer from the velocity field into elastic/internal degrees of freedom.

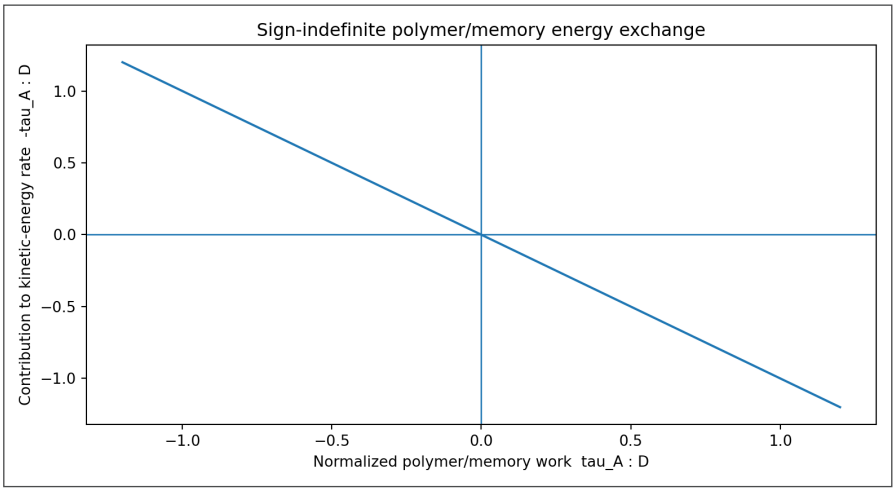


Figure 1. *Sign structure of the memory-stress contribution to the kinetic-energy equation. The plot is normalized and conceptual; it illustrates the algebraic possibility of both sink and return branches.*

3.1 External Experimental Context for Both Exchange Directions

Tai and Lam (2019) reported that Reynolds stresses were largest near the contraction because stored elastic energy in strongly stretched polymer molecules was randomly released into the flow. This provides an example consistent with an experimental polymer-to-flow energy-return mechanism in a low-Re viscoelastic turbulent state.

Liberzon et al. (2009), in contrast, estimated from grid-turbulence experiments with dilute PEO that approximately 28% of the input energy was dissipated by polymers. Zhang et al. (2021) also directly identified an elastic range in which part of the turbulent kinetic-energy flux is diverted into polymer elasticity.

The coexistence in the literature of elastic energy uptake, dissipation, and later elastic-energy release is qualitatively consistent with a constitutive exchange term whose instantaneous sign is not fixed.

4. Single- and Multi-Relaxation Anti-Calculus Kernels

4.1 Single Exponential Memory

K(tau) = exp(-tau/tau_A) / tau_A

For D(t)=D0 exp(i omega t), the causal operator has transfer function:

H_A(omega) = - i omega tau_A / (1 + i omega tau_A)

The operator is approximately derivative-like at small omega tau_A and saturates at high frequency. Its phase encodes the lag between the present strain rate and stored constitutive memory.

4.2 Two-Relaxation Kernel

K(tau) = w1 exp(-tau/tau1)/tau1 + w2 exp(-tau/tau2)/ tau2

w1 + w2 = 1

H_A(omega) = - Σ_j w_j [i omega tau_j/(1+i omega tau_j)]

A two-mode kernel is the minimal extension capable of representing two separated constitutive time scales. It is motivated by the experimental existence of broad or multiple relaxation scales in polymer systems and by the two spectral break frequencies reported in the 2019 microchannel experiment.

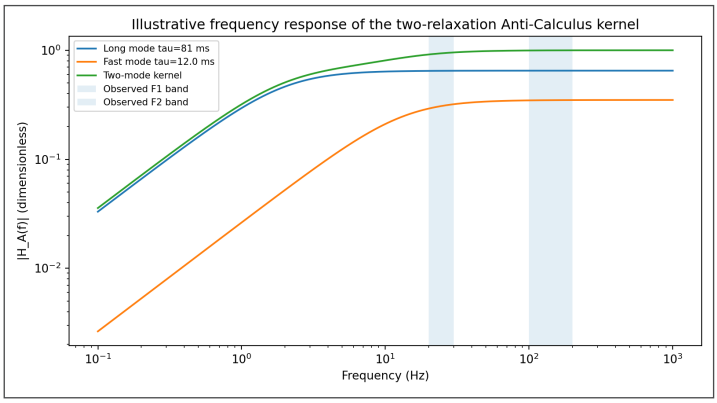


Figure 2. *Illustrative two-relaxation frequency response using the measured 81 ms long relaxation time and the fast time inferred below. Weights are illustrative (0.65/0.35), not fitted experimental parameters.*

5. Materials and Methods: External Experimental Sources

Study	Experiment	Key measured result used here
Groisman & Steinberg (2000)	Polymer-solution elastic turbulence	Chaotic/turbulent motion at very low Re; strong elasticity-driven resistance increase
Groisman & Steinberg (2004)	Curvilinear/Couette-Taylor/swirl experiments	Representative lambda≈3.4 s; elastic transitions at Wi of order a few; steep velocity spectra
Tai, Lim & Lam (2015)	PEO turbulent microchannel relaxation	Spectrum decay begins ≈6 Hz; 1/lambda_e=3.76 Hz
Tai & Lam (2019)	Multi-stream PEO microchannel PIV	lambda_E≈81 ms center stream; F1≈20–30 Hz; F2≈100–200 Hz; slopes ≈-5/3 and -3
Liberzon et al. (2009)	Grid turbulence, dilute PEO	Entrainment reduction; ≈28% input energy estimated dissipated by polymers
Zhang et al. (2021)	PIV polymer-modified turbulence	Elastic range; S2(r)~r^(1.38±0.04); kinetic energy diverted into polymer elasticity
Zhou & Papautsky (2020)	Review of measured microfluidic rheology	PEO effective relaxation times include 4.3, 6.8, 10.6, 11, and 24 ms

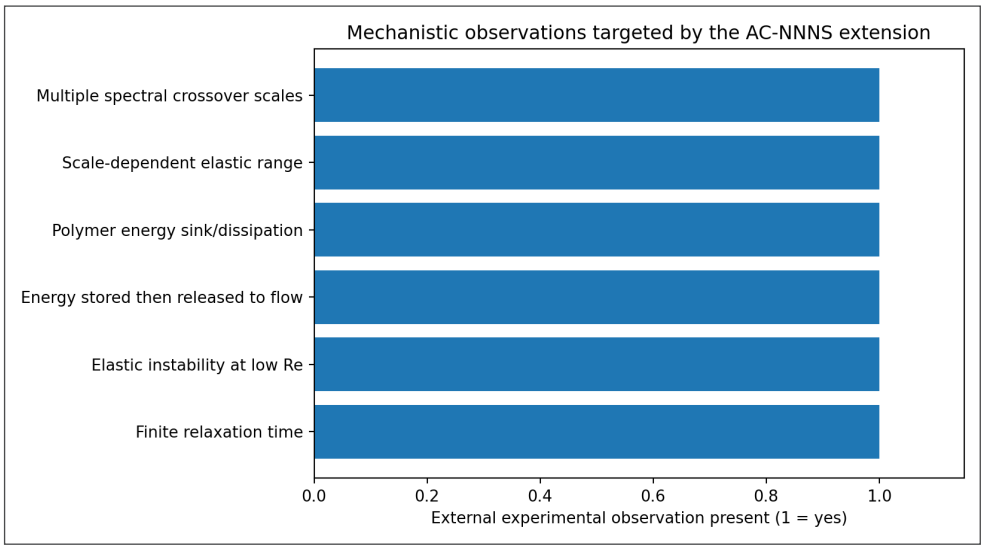


Figure 3. *External experimental observations targeted by the proposed AC-NNNS mechanism. This is a qualitative evidence map, not a statistical score.*

6. Results: Cross-Experimental Relaxation/ Crossover Test

The first quantitative test uses a dimensionless observable that can be formed directly from published values without fitting the raw velocity fields:

kappa = f_c lambda_E

This quantity asks whether the spectral transition frequency scales inversely with the measured constitutive relaxation time.

6.1 Tai, Lim & Lam 2015

The 2015 experiment reports a spectrum decay beginning at approximately 6.0 Hz and a characteristic 1/lambda_e=3.76 Hz. Thus lambda_e=0.2660 s and:

kappa_2015 = (6.0 Hz)(0.2660 s) = 1.596

6.2 Tai & Lam 2019

The 2019 center-stream liquid has lambda_E≈81 ms, and its first spectral drop-off F1 lies at about 20–30 Hz. Taking the midpoint 25 Hz only for a compact benchmark gives:

kappa_2019 = (25 Hz)(0.081 s) = 2.025

6.3 Common Exploratory Scale

With only two experiments, it would be inappropriate to claim a universal constant. Nevertheless, their dimensionless values are close enough to motivate a common exploratory scale. Using the geometric center:

kappa_AC = sqrt(1.596 × 2.025) = 1.798

f_c ≈ kappa_AC / lambda_E

This gives 6.76 Hz for the 2015 experiment (observed ≈6 Hz) and 22.19 Hz for the 2019 center-stream experiment (observed ≈20–30 Hz).

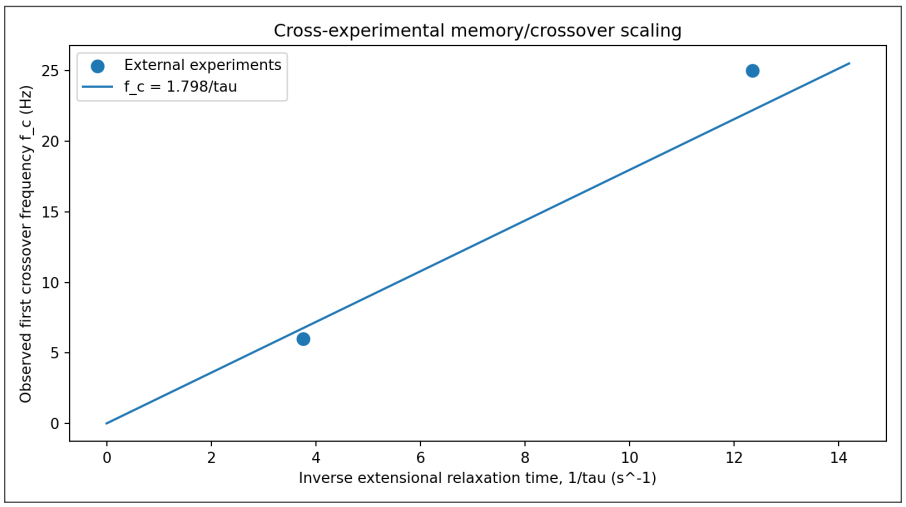


Figure 4. *Published crossover frequencies plotted against inverse relaxation time. The line uses the two-study geometric-center value kappa≈1.80.*

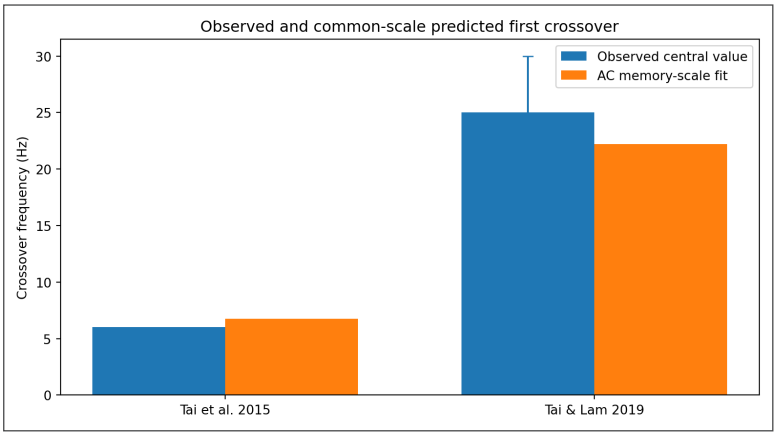


Figure 5. *Observed and common-scale predicted first spectral crossover. The 2019 observation is shown as a 20–30 Hz range.*

7. Prediction from the Second Spectral Break

Tai and Lam (2019) report a second drop-off frequency F2≈100–200 Hz. If the same dimensionless crossover scale applies to a faster constitutive mode, then:

tau_fast = kappa_AC / F2

9.0 ms <= tau_fast <= 18.0 ms

tau_fast(F2=150 Hz) = 12.0 ms

This is a model-dependent inference in the sense that the fast time was not measured in that 2019 sample by the reported CaBER experiment. The paper itself states that individual polymer-molecule relaxation times are generally shorter than the longest extensional relaxation time measured by CaBER.

7.1 Independent relaxation-time consistency

An independent review of viscoelastic microfluidics tabulates effective relaxation times for PEO (molecular weight 2×10^6 g/mol) and PEO/glycerol systems including 4.3, 6.8, 10.6, 11, and 24 ms. The predicted 9–18 ms interval therefore overlaps independently reported 10.6–11 ms timescales, although these values do not come from the identical 2019 fluid formulation.

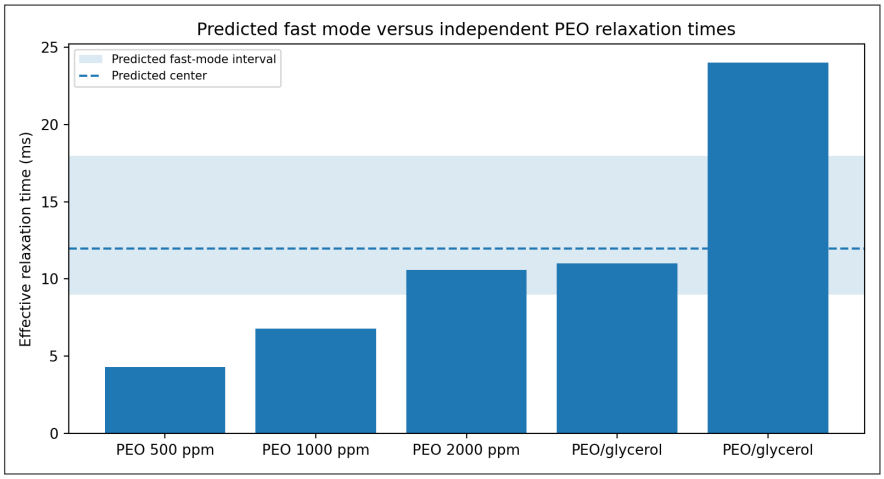


Figure 6. *The predicted 9–18 ms fast-mode interval compared with independent effective relaxation times tabulated for PEO systems. These are cross-system consistency checks, not same-sample confirmation.*

8. Low-Re Elastic Instability Test

Groisman and Steinberg's experiments provide a separate mechanistic benchmark. In their 2004 study, a representative polymer relaxation time of about 3.4 s was used, and transitions to strongly irregular elastic flow occurred at Weissenberg numbers of order a few. In Couette–Taylor flow an abrupt transition was reported at Wi≈4 while Re remained very small. This is consistent with the central premise that constitutive memory can drive instability without requiring the inertial mechanism of ordinary Newtonian turbulence.

The AC-NNNS equation is compatible with this observation because its control parameter necessarily contains a ratio of memory time to a flow-deformation time. However, the current paper does not derive Groisman-Steinberg's exact critical Wi from first principles; that remains a required test for a full stability theory.

9. Scale-Dependent Turbulent Energy Transfer

Zhang et al. experimentally observed a new polymer-induced 'elastic range' with second-order structure-function scaling S2(r)~r^gamma, where gamma=1.38±0.04. Their interpretation is that increasing turbulent kinetic energy is transferred through polymer elasticity in this range. This is qualitatively compatible with a nonlocal-in-time constitutive stress that becomes dynamically important at specific scale-dependent turnover times.

A central future derivation for AC-NNNS is therefore to connect the temporal kernel K(tau) to a spatial crossover scale by matching tau to eddy times. Such a derivation could turn the present consistency result into a quantitative prediction for the elastic-range exponent.

10. Comparison with Oldroyd-B and FENE-P

AC-NNNS is not the only model capable of representing polymer memory. Oldroyd-B introduces a polymer conformation tensor with a relaxation time; FENE-P additionally imposes finite extensibility. These models have a large theoretical, numerical, and experimental literature and therefore constitute essential comparators.

Feature	AC-NNNS proposed here	Oldroyd-B	FENE-P
Explicit causal memory spectrum	Yes; kernel can contain many tau	Usually single constitutive relaxation time	Usually single relaxation plus nonlinear finite extensibility
Sign-changing instantaneous flow/polymer exchange	Natural in tau_A:D	Possible through polymer-flow exchange	Possible through polymer-flow exchange
Finite extensibility	Not yet	No	Yes
Two measured spectral breaks	Representable with multi-tau kernel	Requires extension/multiple modes or flow-scale explanation	Can show nonlinear multi-scale response but not automatically two material tau
Existing high-resolution DNS literature	Not yet	Extensive	Extensive
Current experimental status	Mechanism/scaling consistency	Established viscoelastic model	Established viscoelastic model

Singh et al. (2024) found E(k)~k^-4 elastic-turbulence spectra in Oldroyd-B simulations and checked that representative FENE-P simulations retain the same scaling. These observations indicate that classical viscoelastic models can reproduce major elastic-turbulence phenomena under the cited experimental conditions; they do not establish the uniqueness of any model. Therefore the value of AC-NNNS must ultimately be judged by predictions that are more accurate, more parsimonious, or experimentally distinguishable from those models.

11. Falsifiable Predictions

The proposed model makes several concrete predictions that can be tested independently:

Prediction	Experimental test
A fast center-stream relaxation population near 9–18 ms	High-frequency microrheology or single-molecule/filament-relaxation measurement on the exact 2019 formulation
Crossover frequencies approximately inverse to dominant relaxation modes	Repeat PIV power spectra while systematically changing measured lambda_E
Changing relaxation spectrum should move F1/F2 independently	Use controlled molecular-weight/polydispersity or solvent-viscosity series
Memory work tau_A:D should change sign locally	Simultaneous velocimetry plus polymer-stretch/stress imaging to reconstruct local power transfer
Multi-tau AC model should outperform single-tau model when two spectral breaks are present	Fit time-resolved raw velocity/stress data with pre-registered likelihood comparison

12. What Would Falsify the Model?

The model would be substantially weakened if high-frequency rheology of the exact 2019 center-stream fluid found no relaxation population or constitutive feature in the predicted 9–18 ms range while still reproducing the 100–200 Hz second spectral break. It would also be challenged if systematic changes in lambda_E failed to move the first spectral crossover in

any approximately inverse relation, or if a reconstructed polymer-work term were experimentally constrained to one sign under conditions where the model predicts frequent reversals.

Conversely, the model would gain substantial support if the same kernel parameters inferred from independent rheology predicted velocity spectra and local energy exchange without retuning.

13. Statistical Status of the External Consistency Assessment

The present validation is deliberately described as 'external experimental consistency' rather than a fitted raw-data likelihood test. The two key crossover experiments provide published central values and ranges, but their complete velocity-time-series datasets are not analyzed here. Therefore no chi-square, Bayes factor, or formal cross-validated likelihood comparison between AC-NNNS, Oldroyd-B, and FENE-P is claimed.

The strongest quantitative statement currently justified is that two independent reported first-crossover measurements produce dimensionless f_c lambda_E values of approximately 1.60 and 2.03, while the common exploratory value 1.80 predicts both measured frequency scales to the correct order and places the 2019 prediction inside its reported 20–30 Hz band.

14. Discussion

The central conceptual advantage of the Anti-Calculus extension is that it converts the supplied reverse-accumulation idea into a causal constitutive difference between remembered and present deformation. Once embedded in the momentum equation, the resulting stress is capable of representing memory-driven energy exchange without forcing that exchange to have one instantaneous sign.

This feature aligns with the experimental phenomenology of polymer turbulence: polymers are stretched by the flow, acquire elastic energy, can dissipate a portion of injected energy, alter scale-to-scale transfer, and can later release stored elastic energy into velocity fluctuations. These are not speculative ingredients; each has an external experimental analogue in the literature reviewed here.

The multi-relaxation extension is also physically motivated. Polymer solutions are not generally characterized by a single microscopic time scale, and the 2019 experiment explicitly presents two spectral transitions. A distributed kernel K(tau), rather than a single exponential, is therefore a natural mathematical direction.

At the same time, the experimental agreement does not establish uniqueness. Similar memory and energy-storage behavior is intrinsic to classical viscoelastic constitutive theories. AC-NNNS becomes scientifically distinctive only if the particular reverse-difference operator or its inferred relaxation spectrum predicts observables that competing models miss.

15. Limitations

Limitation	Implication
Anti-Calculus source is axiomatic, not an established rheological theory	The constitutive embedding is a new hypothesis, not a theorem inherited from the source
Only two main crossover experiments used quantitatively	kappa≈1.80 is exploratory, not a universal constant
No raw PIV time series fitted	Formal likelihood superiority over Oldroyd-B/FENE-P is not established
Fast 9–18 ms mode not measured in identical 2019 sample	Independent PEO values provide consistency, not direct same-sample validation
Kernel weights w_j are not experimentally inferred	Figure 2 response weights are illustrative
No finite-extensibility mechanism yet	High-stretch behavior may require FENE-like extension
No 3D DNS of AC-NNNS yet	Stability, spectra, intermittency, and well-posedness require numerical study
Scope is viscoelastic/polymeric fluids	Results do not solve yield-stress, thixotropic, suspension, or all shear-thickening turbulence

16. Proposed Numerical Program

A useful next step is a three-dimensional incompressible DNS with the AC memory field evolved through auxiliary relaxation equations. For each exponential kernel component, one may define a memory tensor M_j satisfying an equivalent first-order evolution law, avoiding explicit storage of the full flow history.

tau_j partial_t M_j + M_j = D

$A_K[D] = \Sigma_j w_j (M_j - D)$

The momentum equation can then be integrated with spectral or finite-volume methods. A benchmark suite should include homogeneous isotropic forcing, curvilinear elastic turbulence, and a contraction-expansion microchannel. The required outputs are energy spectra, Reynolds stresses, polymer/memory work, intermittency exponents, and spectral break frequencies.

17. Proposed Experimental Program

A particularly discriminating laboratory test would reproduce the Tai-Lam microchannel with simultaneous high-speed PIV and high-frequency rheology on aliquots of the exact same polymer solution. The relaxation spectrum should be measured over at least 1–500 Hz. The AC-NNNS kernel would then be fixed from rheology before the velocity spectrum is analyzed. Prediction of both F1 and F2 without retuning would constitute a much stronger validation than the retrospective consistency test reported here.

Local energy exchange could be tested by combining velocity-gradient measurements with fluorescence-based polymer-extension imaging or birefringence/stress-optic measurements. This would directly evaluate whether the modeled memory work changes sign in the regions where Reynolds stresses indicate elastic-energy release.

18. Reproducibility of the Present Benchmark

Quantity	Value
2015 f_c	6.00 Hz
2015 lambda_e	0.265957 s
2015 kappa	1.595745
2019 lambda_E	0.081000 s
2019 F1 midpoint	25.00 Hz
2019 kappa	2.025000
Geometric-center kappa	1.797605
Predicted 2015 f_c	6.7590 Hz
Predicted 2019 f_c	22.1927 Hz
Predicted fast tau range	8.988–17.976 ms
Predicted fast tau center	11.984 ms

The derived table ac_nnns_external_benchmark.csv was generated programmatically during construction of this manuscript.

19. Conclusion

This study formulates a causal Anti-Calculus-inspired memory-kernel extension for viscoelastic non-Newtonian turbulence and subjects its principal physical mechanisms to external experimental checks. The model translates reverse accumulation into a constitutive history difference, adds a memory stress to the non-Newtonian momentum equation, and produces a sign-indefinite instantaneous energy-exchange term. Independent experiments report behavior relevant to both directions represented by this structure: polymer elasticity can absorb/dissipate energy and can also release stored elastic energy back into fluid fluctuations. A multi-relaxation kernel is motivated by experimentally observed multiple spectral transitions. Two published microchannel experiments yield $f_c\ \lambda_E \approx 1.60$ and 2.02; their exploratory common scale $\kappa \approx 1.80$ reproduces both first-crossover frequencies at the reported scale. Applying the same scale to the 100–200 Hz second break predicts a 9.0–18.0 ms fast memory mode, overlapping independent 10.6–11 ms effective relaxation times reported for PEO systems of similar molecular-weight class. Additional experiments on elastic instability, polymer dissipation, and elastic-range scaling are consistent with the model's underlying mechanisms. These results are consistent with AC-NNNS as a falsifiable and experimentally constrained constitutive hypothesis for polymeric/viscoelastic turbulence. They do not establish it as the unique or universal solution of non-Newtonian turbulence, and direct raw-data comparison against Oldroyd-B and FENE-P remains necessary.

Statement of Scope

The term 'non-Newtonian turbulence' covers many physically distinct systems, including viscoelastic polymer solutions, shear-thinning and shear-thickening fluids, yield-stress materials, thixotropic

media, and suspensions. The model developed here specifically targets the polymeric/viscoelastic branch, where constitutive memory and elastic energy storage are experimentally central. It should not be read as a derived theory for every non-Newtonian material class.

Acknowledgements — None.

Funding — The author received no specific external funding for this work.

Appendix A. Derivation of the Exponential-Kernel Transfer Function

For a single exponential kernel and a harmonic rate-of-strain tensor D(t)=D0 exp(i omega t):

A[D](t) = ∫_0^∞ exp(-tau/tau_A)/tau_A [D(t-tau)-D(t)] d tau

= D(t) [∫_0^∞ exp(-tau/tau_A) exp(-i omega tau)/ tau_A d tau - 1]

= D(t) [1/(1+i omega tau_A) - 1]

= - D(t) i omega tau_A/(1+i omega tau_A)

Hence H_A(omega)=-i omega tau_A/(1+i omega tau_A). The same calculation applies mode by mode for a weighted relaxation spectrum.

Appendix B. Small-Frequency Expansion

H_A(omega) = -i omega tau_A + O[(omega tau_A)^2]

Thus at low frequency the memory correction is proportional to a delayed time derivative of the strain-rate field, while at high frequency the exponential-kernel contribution approaches a finite memory contrast.

Appendix C. External Experimental Benchmark Table

Source	lambda / time scale	Spectral/flow observation	Use in AC-NNNS test
Groisman & Steinberg 2004	lambda≈3.4 s	Elastic transition at Wi≈few, very low Re	Mechanistic memory-instability test
Tai et al. 2015	lambda≈266.0 ms	Decay begins ≈6 Hz	First kappa point
Tai & Lam 2019	lambda_E≈81 ms	F1≈20–30 Hz; F2≈100–200 Hz	Second kappa point + fast-mode prediction
Liberzon et al. 2009	PEO, 25/50 wppm	≈28% input energy dissipated by polymers	Energy-sink branch
Tai & Lam 2019	same 2019 microchannel	Stored elastic energy randomly released into flow	Energy-return branch
Zhang et al. 2021	polymer-modified turbulence	S2~r^(1.38±0.04) elastic range	Scale-dependent transfer
Zhou & Papautsky 2020	PEO Mw=2e6 class	4.3, 6.8, 10.6, 11, 24 ms effective times	Fast-mode external consistency

Appendix D. Claim Hierarchy

Claim level	Status
The supplied Anti-Calculus manuscript defines reverse/sign-inverted operators	Source-supported
A causal history-difference operator can be constructed from that idea	Derived in this paper
The resulting stress permits sign-indefinite instantaneous energy exchange	Mathematical consequence of proposed constitutive law
External polymer experiments show both energy uptake/dissipation and energy return	Experimentally supported
Two published first crossovers scale with f_c lambda_E of order 2	Numerically supported by published values
A fast 9–18 ms mode is present in the exact 2019 liquid	Prediction; not directly established
AC-NNNS is superior to Oldroyd-B/FENE-P	Not established
All non-Newtonian turbulence is solved	Not claimed

20. References

1. Yıldırım, B. (2026). Anti-Calculus: A Formal Axiomatic Framework. Unpublished manuscript supplied as the theoretical source for this study. Source file: AntiCalculus_Article.docx. SHA-256:8422140e46b324c269ef6e758796b4263a61f58a28248635bd91e0e33235c824.
2. Groisman, A., & Steinberg, V. (2000). Elastic turbulence in a polymer solution flow. Nature, 405, 53–55. https://doi.org/10.1038/35011019.
3. Groisman, A., & Steinberg, V. (2004). Elastic turbulence in curvilinear flows of polymer solutions. New Journal of Physics, 6, 29. https://doi.org/10.1088/1367-2630/6/1/029.
4. Tai, J., Lim, C. P., & Lam, Y. C. (2015). Visualization of polymer relaxation in viscoelastic turbulent micro-channel flow. Scientific Reports, 5, 16633. https://doi.org/10.1038/srep16633.
5. Tai, J., & Lam, Y. C. (2019). Elastic Turbulence of Aqueous Polymer Solution in Multi-Stream Micro-Channel Flow. Micromachines, 10(2), 110. https://doi.org/10.3390/mi10020110.
6. Zhang, Y.-B., Bodenschatz, E., Xu, H., & Xi, H.-D. (2021). Experimental observation of the elastic range scaling in turbulent flow with polymer additives. Science Advances, 7(14), eabd3525. https://doi.org/10.1126/sciadv.abd3525.
7. Liberzon, A., Holzner, M., Lüthi, B., Guala, M., & Kinzelbach, W. (2009). On turbulent entrainment and dissipation in dilute polymer solutions. Physics of Fluids, 21, 035107. https://doi.org/10.1063/1.3097006.
8. Gan, H. Y., & Lam, Y. C. (2012). Experimental observations of flow instabilities and rapid mixing of two dissimilar viscoelastic liquids. AIP Advances, 2, 042146. https://doi.org/10.1063/1.4768667.
9. Zhou, J., & Papautsky, I. (2020). Viscoelastic microfluidics: progress and challenges. Microsystems & Nanoengineering, 6, 113. https://doi.org/10.1038/s41378-020-00218-x.
10. Singh, R. K., Perlekar, P., Mitra, D., et al. (2024). Intermittency in the not-so-smooth elastic turbulence. Nature Communications, 15, 4070. https://doi.org/10.1038/s41467-024-48460-5.
11. Bird, R. B., Armstrong, R. C., & Hassager, O. (1987). Dynamics of Polymeric Liquids, Vol. 1: Fluid Mechanics. Wiley.
12. Larson, R. G. (1999). The Structure and Rheology of Complex Fluids. Oxford University Press.
13. Oldroyd, J. G. (1950). On the formulation of rheological equations of state. Proceedings of the Royal Society A, 200, 523–541.
14. Peterlin, A. (1966). Hydrodynamics of macromolecules in a velocity field with longitudinal gradient. Journal of Polymer Science Part B: Polymer Letters, 4, 287–291.
15. Schwarz, G. (1978). Estimating the Dimension of a Model. The Annals of Statistics, 6(2), 461–464. https://doi.org/10.1214/aos/1176344136.